



# Application of an electrochemical sensor using copper oxide nanoparticles/polyalizarin yellow R nanocomposite for hydrogen peroxide

Nader Amini<sup>1</sup> · Bahaaldin Rashidzadeh<sup>2</sup> · Nasrin Amanollahi<sup>2</sup> · Afshin Maleki<sup>1</sup> · Jae-Kyu Yang<sup>3</sup> · Seung-Mok Lee<sup>4</sup>

Received: 16 July 2020 / Accepted: 1 March 2021 / Published online: 19 March 2021  
© Springer-Verlag GmbH Germany, part of Springer Nature 2021

## Abstract

In this study, copper oxide nanoparticles (CuONPs) were prepared by a simple chemical method and then characterized by scanning electron microscope (SEM). A novel electrochemical sensor for hydrogen peroxide (H<sub>2</sub>O<sub>2</sub>) analysis was prepared by immobilizing copper oxide nanoparticles and polyalizarin yellow R (PYAR) on bare glassy carbon electrode (PAYR/CuONPs/GCE). The electrocatalytic behavior of the proposed electrochemical sensor was also studied by cyclic voltammetry (CV), electrochemical impedance spectroscopy (EIS), and differential pulse voltammetry (DPV). Based on the results, the PAYR/CuONP nanocomposite had significant electrocatalytic oxidation and reduction properties for the detection and determination of H<sub>2</sub>O<sub>2</sub>. Some parameters such as linear range, sensitivity, and detection limit for reduction peak were obtained as 0.1–140 μM, 1.4154 μA cm<sup>-2</sup> μM<sup>-1</sup>, and 0.03 μM, respectively, by the DPV technique. Some advantages of this electrode were having widespread linear range, low detection limit, and, most importantly, ability in simultaneous oxidation and reduction of H<sub>2</sub>O<sub>2</sub> at two applied potentials.

**Keywords** Electrochemical sensor · Hydrogen peroxide · Nanocomposite · Copper oxide nanoparticles · Polyalizarin yellow R

## Introduction

Hydrogen peroxide (H<sub>2</sub>O<sub>2</sub>) has been widely applied in various fields such as paper and textile bleaching, microbial control characteristics, foodstuff, environmental approaches, cosmetics,

and pharmaceutical activities [Pandurangan et al. 2014; Thanh et al. 2016]. Furthermore, H<sub>2</sub>O<sub>2</sub> is widely used to oxidize cellulose, recycle wastepaper, treat wastewaters, boost rocket fuels, produce a variety of chemicals and plastics, and detoxify organic pollutants that might contaminate the environment [Marjan et al. 2019]. It is also an essential material in several enzymatic reactions in the biological system [Zhang and Chen 2017]. The H<sub>2</sub>O<sub>2</sub> layer is the first defense of the immune system against various pathogens. However, the surplus leakage of H<sub>2</sub>O<sub>2</sub> in biological species has a harmful effect on the body which can cause irritation of stomach and skin as well as damage to the gastrointestinal tract and proteins [Yusoff et al. 2017]. Moreover, it has been documented that excess amounts of this compound in the body causes a variety of diseases such as DNA fragmentation, Alzheimer's, Parkinson's, diabetes, membrane damage, neurodegeneration, tissue damage, cancer, cardiovascular, and aging problems (Sahoo et al. 2020; Lutfullah and Muhammet 2019). Furthermore, according to the US Food and Drug Administration (FDA), the H<sub>2</sub>O<sub>2</sub> tolerance limit as an anti-microbial agent for vegetables, fruits, herbs, and spices is 120 mg/L [Parthasarathy et al. 2016]. Therefore, the determination of H<sub>2</sub>O<sub>2</sub> is of great importance in both biological and environmental processes. There are several analytical techniques

Responsible Editor: Angeles Blanco

- ✉ Nader Amini  
naderamini95@yahoo.com
- ✉ Bahaaldin Rashidzadeh  
b\_rashidzadeh@pnu.ac.ir
- ✉ Jae-Kyu Yang  
jkyang@kw.ac.kr

- <sup>1</sup> Environmental Health Research Center, Research Institute for Health Development, Kurdistan University of Medical Sciences, Sanandaj, Iran
- <sup>2</sup> Department of Chemistry, Payamenoor, Tehran 19395-4697, Iran
- <sup>3</sup> Department of Environmental Engineering, Kwangwoon University, Seoul 01897, South Korea
- <sup>4</sup> Department of Biosystems and Convergence Engineering, Catholic Kwandong University, 25601 Gangneung, South Korea

such as spectroscopy and chromatography which are available for the determination of  $\text{H}_2\text{O}_2$ . However, these methods require much time as well as a lot of cost and show poor repeatability [Liu et al. 2017; Wu et al. 2017]. Compared to previous techniques, electrochemical tools have much attention from researchers owing to their simplicity, low cost, low detection limit, and high sensitivity. Moreover, in both enzymatic and non-enzymatic processes, electrochemical methods are feasible [Devasenathipathy et al. 2016; Wang et al. 2011].

The electrochemical determination of hydrogen peroxide on the surface of bare electrodes is a very slow process. To solve this problem, the surface of these electrodes should be modified using various compounds such as enzymes [Díaz Nieto et al. 2018], conductive polymers [Zhang et al. 2011], and metals and bimetals [Devasenathipathy et al. 2016; Chao et al. 2016; Chen et al. 2016; Ensafi et al. 2016; Sookhakian et al. 2017; Abdelwahab and Shim 2014; Guler et al. 2018]. The literature review revealed that metal oxide-based electrochemical sensors such as NiO, ZnO,  $\text{Fe}_2\text{O}_3$ ,  $\text{Co}_3\text{O}_4$ , and CuO have some advantages such as ease of preparation, low cost, good electrocatalytic properties, and capability of conducting electrochemical reactions at lower potentials. Among them, copper oxide is one of the best materials due to its excellent redox property, non-toxicity, and high stability and conductivity [Xie et al. 2018; Ehsani et al. 2017; Kardaş et al. 2017]. Conducting polymers have been used as a modifier for fabrication of electrochemical sensors [Doblhofer 1980]. These polymers have the benefits of good stability, high conductivity, and considerable stability on the surface of electrodes. Some specific monomers of these polymers have been applied to prepare electrochemical sensors such as neutral red [Shobha Jeykumari and Narayanan 2008; Yogeswaran and Chen 2007; Zhang and Zhang 2010], toluidine blue [Zeng et al. 2006], alizarin red S [Wu and Hu 2004], Congo red [Hu et al. 2006, 2007a, b], Nile blue A [Du et al. 2008], thionine [Zhang et al. 2010], pyrocatechol violet [Sheng et al. 2007], and alizarin yellow R [Zhang et al. 2011]. The formed composite film through amalgamating conductive polymers with other materials such as nanoparticles as a modifier is proposed for the construction of these sensors. For instance, carbon nanotube/poly (alizarin red S) and multiwall carbon nanotube/alizarin were used for detection of nitrite and kojic acid, respectively [Yue et al. 2010; Liu et al. 2009]. One of the conductive polymers is alizarin yellow R (AYR) and is applied as a pH and metallochromic indicator [Williams and Lautenschleger 1963; Ihara et al. 2008]. Therefore, in the current research, an electrode modified with CuO nanoparticles and polyalizarin yellow R was fabricated for hydrogen peroxide monitoring. The combination of polyalizarin yellow R (a conductive polymer on the electrode surface) and CuONps (high surface and conductivity) exhibited excellent electrocatalytic activity for the electrooxidation and electroreduction of hydrogen peroxide. This proposed electrochemical sensor was

applied to detect and determine hydrogen peroxide in milk samples with satisfactory results.

## Materials and methods

### Materials

Hydrogen peroxide, copper (II) sulfate pentahydrate, alizarin yellow R, hydrochloric acid (HCl), phosphoric acid ( $\text{H}_3\text{PO}_4$ ), sodium sulfate ( $\text{Na}_2\text{SO}_4$ ), sodium hydrogen phosphate, and sodium hydroxide (NaOH) were obtained from Merck.

### Apparatus

All experiments and electrochemical measurements were performed using a  $\mu$ -autolab device (model 101 made by Metrohm). A three-electrode system consisting of a platinum (Pt) counter electrode, a glassy carbon working electrode (GCE), and an Ag/AgCl[KCl(sat)] reference electrode was placed in the electrochemical cell.

### Preparation of copper oxide nanoparticles (CuONPs)

The copper oxide nanoparticles were prepared by a simple chemical technique. First, 1 mL of  $\text{Na}_2\text{SO}_4$  (0.1 M) was added to 17 mL of  $\text{CuSO}_4$  (0.005 M), and then mixed well and shaken for 120 min at 25 °C.

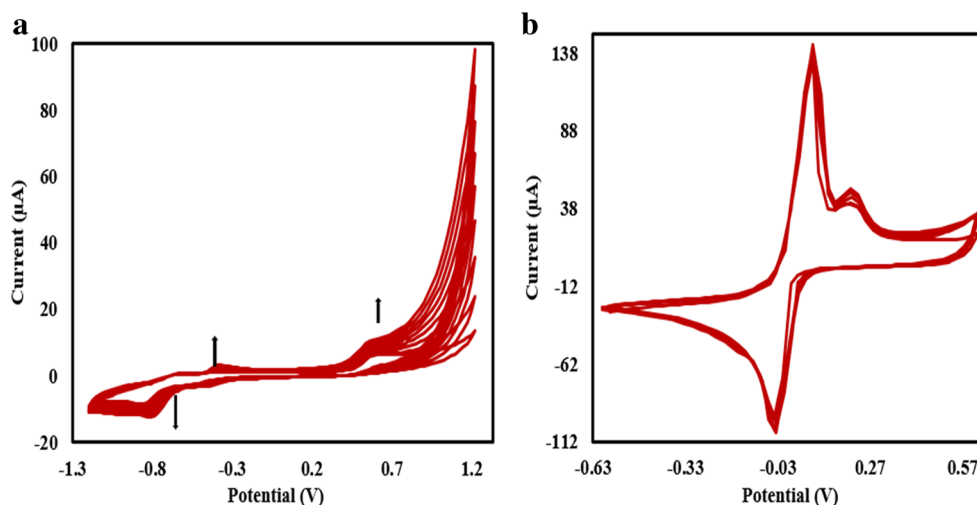
### Construction of the modified electrode

The bare glassy carbon electrode was polished continuously using sandpaper (nos. 1–6) and 0.5 mm of alumina slurry to remove contaminants from the electrode surface. Next, the surface of the electrode was sonicated in a mixture of ethanol and distilled water for 5 min to remove adsorbed particles and then washed using distilled water. For the modification of the electrode, the electropolymerization of alizarin yellow R (1 mM) was carried out in the range of potential  $-1.0$  to  $1.2$  V at a scan rate 100 mV/s and at pH 12 (Fig. 1).

The reduction and oxidation peak currents increased with continuous scanning number (20 cycles), illustrating the successive growth of alizarin yellow R on the surface of the glassy carbon electrode.

For the fabrication of PYAR/CuONPs/GCE, the PYAR/GCE was immobilized in a mixture of  $\text{Na}_2\text{SO}_4$  and  $\text{CuSO}_4$ . Then, the cyclic voltammetry (CV) method was applied under 10 scanning cycles at the potential range between  $-1$  and  $+1$  V and at a scan rate of 100 mV/s for depositing CuO nanoparticles on the surface of the electrode (Fig. 1B).

**Fig. 1** (A) The continuous CVs of the alizarin yellow R electropolymerization on GCE at pH 12 at scan rate  $100 \text{ mVs}^{-1}$ . (B) Cyclic voltammograms of copper oxide (CuO) electrodepositing



### Characterization of poly (alizarin yellow R)-CuONPs/GCE

Figure 2A shows the SEM image of the synthesized nanoparticles. The average particle size was less than 70 nm, which lies in the range of nanomaterials.

## Results and discussions

### Electrochemical characterization of PYAR/CuONPs/GC electrode

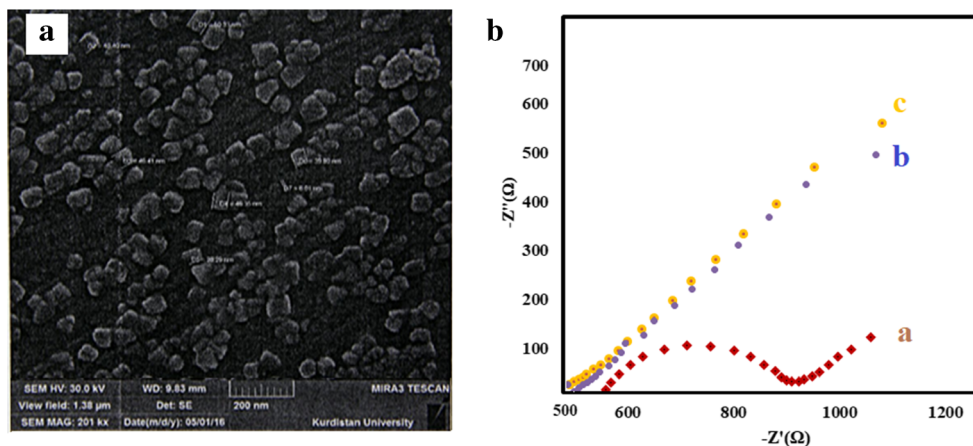
In order to obtain information of electrochemical characterization as well as study electrochemical manner through the step-by-step promotion process of the modification, electrochemical impedance spectroscopy (EIS) was applied. In the EIS technique, the  $R_{ct}$ ,  $C$ , and  $R_s$  symbols are charge transfer resistance, double-layer capacitance, and solution resistance, respectively.

Figure 2B indicates the impedance spectra depicted as Nyquist plots ( $Z_{im}$  vs.  $Z_{re}$ ) for diverse electrodes as bare GCE (a), polyalizarin yellow R/GCE (b), and CuONPs/polyalizarin yellow R/GCE (c) in 5 mM  $\text{Fe}(\text{CN})_6^{3-/4-}$  probe in the frequency range of 0.01 to  $10^4$  Hz.

Based on the EIS curves, the semicircle portion with respect to electron transfer is a limited process and its diameter is equal to the electron transfer,  $R_{ct}$ , which controls electron transfer kinetics of redox probe on the electron interface. The EIS data of the electrodes were placed on a simple circuit which is exhibited in the plot (Fig. 2B. Inset).

It can be observed from the Nyquist schemes (Fig. 2B) that the semicircle of the bare electrode indicates a diffusion restrictive stage of the electrochemical procedure and dramatical reduction in polyalizarin yellow R/GCE. Once the polyalizarin yellow R/CuONP nanocomposite was immobilized on the electrode surface, the EIS curve's diameter became smaller than that of other electrodes. These results show that electron transfer is easy between the electrode surface and solution in polyalizarin yellow R/CuONPs/GCE. It indicates that

**Fig. 2** (A) SEM image of CuO nanoparticles. (B) Electrochemical impedance spectroscopy (EIS), (a) bare GCE, (b) polyalizarin /GCE, (c) CuONPs/polyalizarin/GCE in 5 mM probe  $\text{Fe}(\text{CN})_6^{4-/3-}$



polyalizarin yellow R/CuONPs increase electron transfer and exhibit formation of a new layer on the substrate.

### Electrocatalytic oxidation and reduction of hydrogen peroxide on poly (alizarin yellow R)-CuONPs/GCE

Cyclic voltammetry was utilized for investigating electrooxidation and electroreduction of hydrogen peroxide on the surface of unmodified and modified electrodes. Figure 3 shows that no peaks were discerned from the bare GC electrode (a), modified electrode by alizarin yellow polymer (b), modified electrode by the CuO nanoparticles, and alizarin yellow polymer (c) in the absence of hydrogen peroxide. In addition, no peaks were observed for the unmodified electrode in the presence of hydrogen peroxide (d). These findings indicate that hydrogen peroxide on the surface of the bare electrode was not capable of direct electron transfer. By contrast, on the surface of modified electrode by polyalizarin yellow (e), a pair of redox peaks were detected in the presence of hydrogen peroxide, suggesting that the polyalizarin yellow might be involved in direct electron transfer of hydrogen peroxide. Finally, a pair of redox peaks were clearly seen in the presence of hydrogen peroxide on the surface of the modified electrode with the CuO nanoparticles and polyalizarin yellow (f). This result suggests that the dramatic increase of simultaneous oxidation and reduction currents of hydrogen peroxide and, in turn, the potential of simultaneous oxidation and reduction shifted to less positive and less negative amounts, respectively. In general, the electrical conductivity induced by alizarin yellow polymer increased in the presence of the CuO nanoparticles with a high surface area

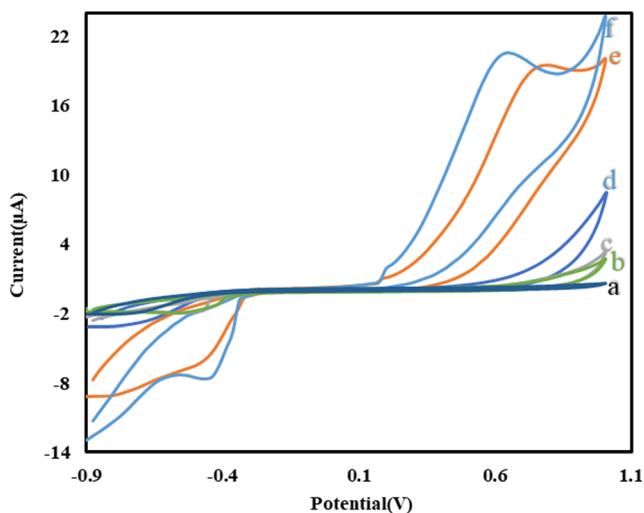


**Fig. 3** Cyclic voltammograms of glassy carbon electrodes modified by CuO nanoparticles and alizarin yellow (f), alizarin yellow (e), and unmodified (d), in the presence of 0.001 M hydrogen peroxide, as well as modified by CuO nanoparticles and alizarin yellow (c), alizarin yellow (b), non-modified (a), in absence of hydrogen peroxide at pH = 10 and scan rate 30 mV/s

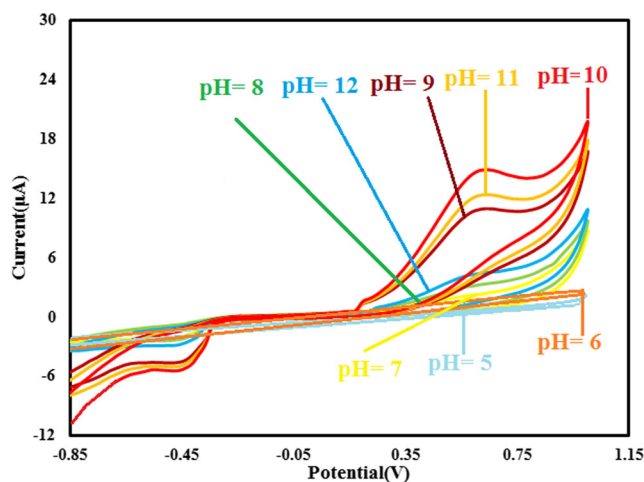


**Fig. 4** Cyclic voltammograms of modified electrode in different pH solutions in the presence of hydrogen peroxide

of the modified electrode which facilitates the transport of direct electrons between hydrogen peroxide and surface of the modified electrode.

In order to investigate the electrocatalytic behavior and an optimal pH of polyalizarin yellow R/CuONPs/GCE, the effect of pH on the electrooxidation and electroreduction responses of this electrode in the presence of hydrogen peroxide between  $-0.9$  and  $+1.1$  V at a scan rate of 100 mV/s was evaluated (Fig. 4).

In acidic medium, no peak of oxidation or reduction of hydrogen peroxide was observed. However, only a peak of reduction was observed in neutral medium (pH 7). Moreover, at pH 8, the oxidation and reduction peak currents were very low. At pH 12–14, the electrodes were damaged and the modifiers were removed from the electrode surface. At pH 10 and 11,  $E_{pa}$  and  $E_{pc}$  were 0.63 and  $-0.43$  V, respectively. And, at pH 10,  $I_{pa}$  and  $I_{pc}$  were 14.92 and  $-5.42$   $\mu\text{A}$ , respectively. But, at pH 11,  $I_{pa}$  and  $I_{pc}$  were 10.38 and  $-5.15$   $\mu\text{A}$ , respectively. As both of the oxidation and reduction peak currents at pH 10 were higher than that at pH 11, pH 10 was selected as the optimum value.

Scan rate effect is a technique for evaluating the process controlled by diffusion as expected in a catalytic system. Figure 5A illustrates the proposed electrode in the presence of 500  $\mu\text{M}$  hydrogen peroxide and scanning rates between 10 and 1000 mV/s. As observed in Figs. 5B and 5C, there is a linear relationship between anodic/cathodic peak currents of hydrogen peroxide and the square root of the scan rate, confirming the diffusion of the process.

The performance of the proposed modified electrode (PAYR/CuONPs/GCE) in the presence of hydrogen peroxide (at various contents) was studied (Fig. 6A). As shown, this electrode has a rapid response and good sensitivity for electroreduction and electrooxidation of hydrogen peroxide. According to Figs. 6B and 6C, a linear relationship between the amount of hydrogen peroxide concentration and the current of anodic and cathodic peaks was observed.

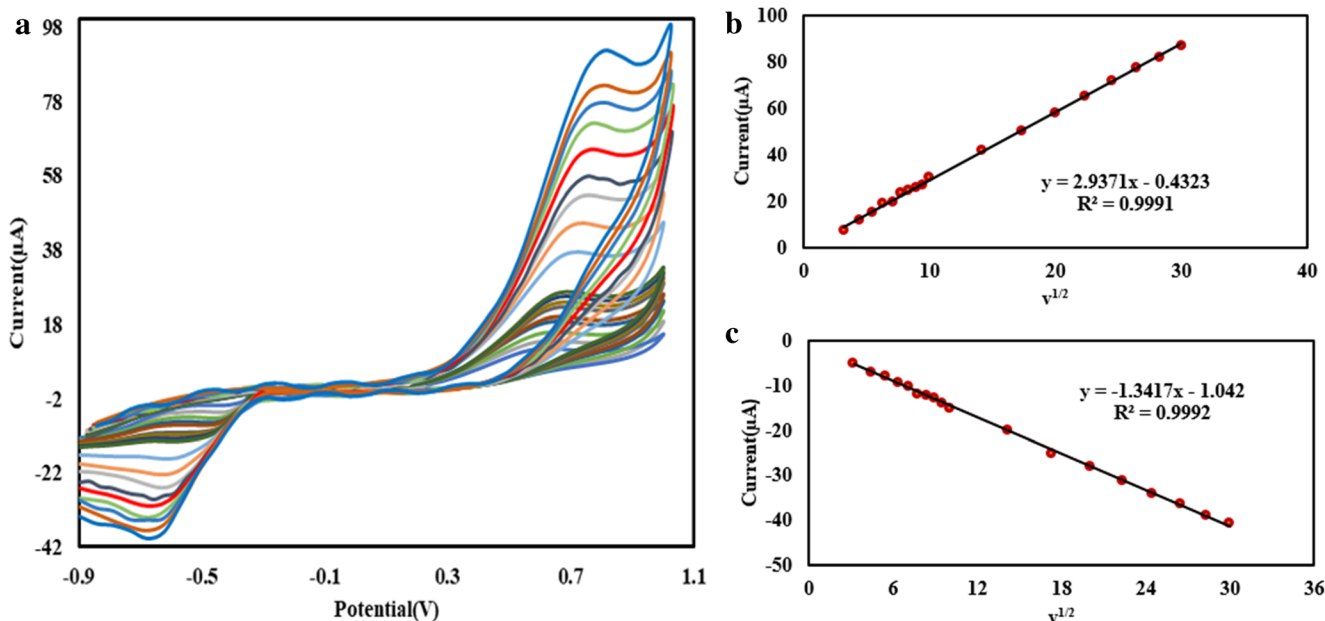
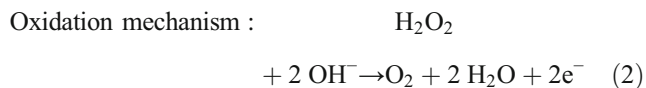
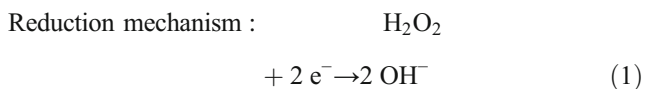


**Fig. 5** (A) Cyclic voltammograms of modified electrode in the presence of 100 μL of hydrogen peroxide (0.001 M) in phosphate buffer solution at pH = 10 at different scanning rates, (B) plot of peak current vs.  $v^{1/2}$  for oxidation peak, (C) plot of peak current vs.  $v^{1/2}$  for reduction peak

Detection limit, sensitivity, and linear range for oxidation and reduction peaks were calculated (Table 1). Based on the results, the oxidation and reduction mechanism of hydrogen peroxide is proposed as follows:



In order to achieve a lower detection limit, differential pulse voltammetry (DPV) was used. The differential pulse voltammograms of the modified electrode at various concentrations of hydrogen peroxide are presented at pH 10 (Fig. 7A)

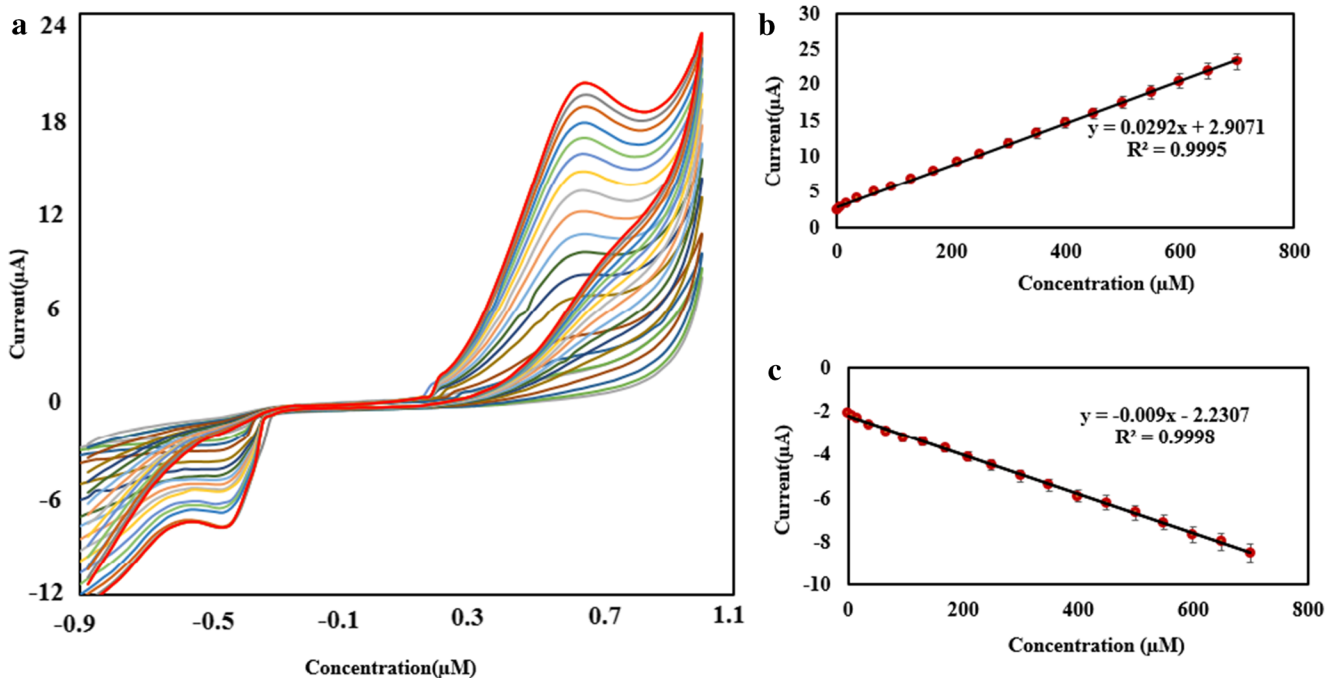


**Fig. 6** (A) Cyclic voltammograms of modified electrode in phosphate buffer solution at pH = 10 at concentrations of 1 and 5 to 700 μM of hydrogen peroxide, (B) plot of peak current vs. hydrogen peroxide concentrations: the oxidation current, (C) and the reduction current

**Table 1** Analytical parameters of several sensors for determination of H<sub>2</sub>O<sub>2</sub>

Electrode	LOD ( $\mu\text{M}$ )	Linear range ( $\mu\text{M}$ )	Sensitivity ( $\mu\text{A cm}^{-2} \mu\text{M}^{-1}$ )	Ref
MnS@MoS <sub>2</sub>	0.12	0.5–5000	0.650	Priyanga et al. 2021
C <sub>rod</sub> @Ag	100	500–5000	0.128	Agnieszka et al. 2021
CoFe <sub>2</sub> O <sub>4</sub> /CNTs	0.02	5–100	14.1	Sahoo et al. 2020
AgNp@GNR	20	50–5000	-	Vesna et al. 2020
Pd@CeO <sub>2</sub> NH <sub>2</sub>	0.47	3200–17,500	85.265	Muhammet et al. 2018
CoSn(OH) <sub>6</sub>	1	4–400	0.01935	Shu et al. 2017
Gr-CCS-AgNPs	2.49	20–5020	-	Wang et al. 2017
MnOOH/CC	3.2	200–9670	692.42	Weina et al. 2016
PAYR/CuONPs (DPV-reduction peak)	0.03	0.1–140	1.4154	This work
PAYR/CuONPs (CV-reduction peak)	0.28	1–700	0.009	This work
PAYR/CuONPs (CV-oxidation peak)	3	5–700	0.0292	This work

because the detection limit of the reduction peak is low in the cyclic voltammetry method. Therefore, in the differential pulse voltammetry method, the reduction peak is investigated.

Figure 7B indicates that the intensity of the cathodic peak increased by increasing the concentration of hydrogen peroxide. A linear dependence of the catalytic currents vs. hydrogen peroxide concentration can be shown in the equation  $I (\mu\text{A}) = 1.4154 (\text{hydrogen peroxide}) \mu\text{A} \mu\text{M}^{-1} + 0.4607 \mu\text{A}$ . Table 1 presents the detection limit, sensitivity, and linear range for reduction peaks.

### Comparison of PAYR/CuONPs/GCE with those of previous modified electrodes

The proposed sensor was compared with several other electrochemical sensors that have been applied for hydrogen peroxide analysis. Table 1 demonstrates that some electrochemical parameters such as linear range, lower detection limit, and

sensitivity of PAYR/CuONPs/GCE are better or comparable with those of other sensors.

### Repeatability, stability, and selectivity

For five consecutive assays, the repeatability of the modified electrode response current in the presence of 500  $\mu\text{M}$  of hydrogen peroxide was assessed. The variation coefficient (R.S.D) was 3.75%. To study the lifetime and stability of the proposed sensor, the sensor response current after 1 and 5 weeks was calculated. After this time, the observed reductions in the electrode response were approximately 96.5 and 88.5% of the initial currents, respectively. Furthermore, the interference effect of l-cysteine, glucose glycine, fructose, mannose, arginine, phenylalanine, Na<sup>+</sup>, K<sup>+</sup>, Mg<sup>+2</sup>, and Ca<sup>+2</sup> in the presence of H<sub>2</sub>O<sub>2</sub> on the proposed sensor response was investigated by the DPV method. According to the experimental results, glycine, fructose, mannose, arginine, phenylalanine, Na<sup>+</sup>, K<sup>+</sup>,

**Fig. 7** (A) Differential pulse voltammetry of modified electrode at pH 10 with increasing of hydrogen peroxide concentrations. (B) Plots of peak current vs. H<sub>2</sub>O<sub>2</sub> concentrations

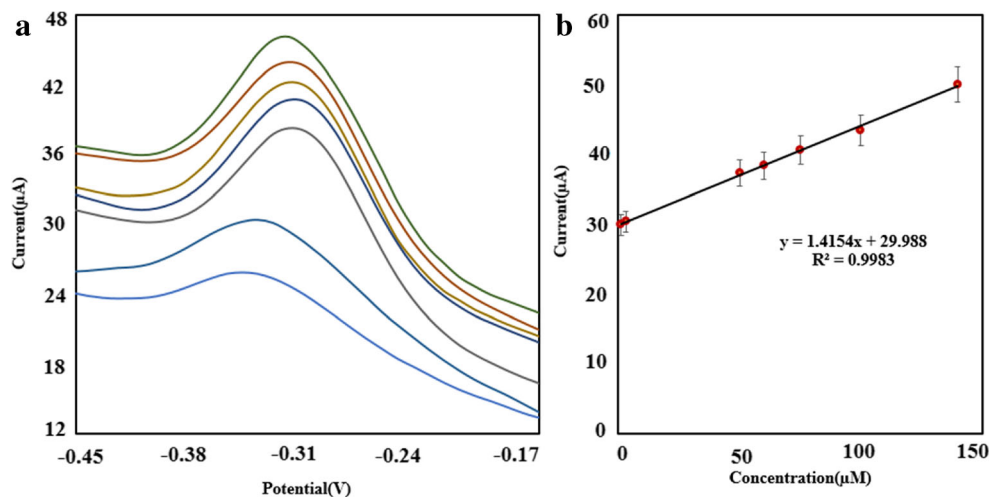


**Table 2** Determination of H<sub>2</sub>O<sub>2</sub> in milk samples

Sample	Added (μM)	Found (μM)	Recovery (%)
1	50	59	100.8
	150	152	101.3
2	50	48.5	97
	150	153.3	102.3

Mg<sup>+2</sup>, and Ca<sup>+2</sup> did not interfere in determination of H<sub>2</sub>O<sub>2</sub> with 10 folds excess over H<sub>2</sub>O<sub>2</sub> concentration. The interference for l-cysteine and glucose appeared in equimolar concentration in the solution with H<sub>2</sub>O<sub>2</sub>.

### Analytical application

To analyze the real samples, the reduction peak was selected. The practicality of the present sensor was appraised for the detection of H<sub>2</sub>O<sub>2</sub> in different milk samples through the CV method. H<sub>2</sub>O<sub>2</sub> concentration was measured in two diverse milk samples provided from a store. The samples were prepared with 50 μM and 150 μM of H<sub>2</sub>O<sub>2</sub> and the content of hydrogen peroxide recovery was calculated. The hydrogen peroxide concentration was specified in all the samples through the method described in Table 2. A blank milk sample was tested in a similar way and showed no meaningful current response. According to Table 2, it is apparent that this sensor showed rational selectivity in the case of the real milk samples and generated acceptable outcomes with the recoveries ranging from 97 to 102.3%.

### Conclusion

In the present work, a new strategy was applied for the fabrication of alizarin yellow-based CuO nanoparticles via electrochemical techniques. A novel modified electrode based on polyalizarin/CuONPs immobilized on the surface of glassy carbon electrode was developed and applied. The electrooxidation and electroreduction of H<sub>2</sub>O<sub>2</sub> on the surface of the modified electrode were investigated. The suggested electrode can be applied for the detection of low levels of H<sub>2</sub>O<sub>2</sub>. The assembly of the metal oxide nanoparticles by the conductive polymer yields novel nanocomposite with synergistic properties and functions. This method is useful for novel sensor and biosensor construction.

**Author contribution** Nader Amini performed detection and determination of H<sub>2</sub>O<sub>2</sub> using an electrochemical sensor. Bahaaldin Rashidzadeh, Nasrin Amanollahi, and Afshin Maleki evaluated the experimental data and analysis of the data set. Jae-Kyu Yang and Seung-Mok Lee provided guidance on the preparation method of the electrochemical sensor.

**Funding** This work was partially supported by Kwangwoon University, Seoul, Korea, through Research Grant–2021.

**Data Availability** The data sets used and/or analyzed during the current study are available from the corresponding author (Nader Amini) on reasonable request.

### Declarations

**Ethics approval and consent to participate** Not applicable.

**Consent for publication** Not applicable.

**Conflict of interest** The authors declare no competing interests.

### References

- Abdelwahab AA, Shim YB (2014) Nonenzymatic H<sub>2</sub>O<sub>2</sub> sensing based on silver nanoparticles capped polyterthiophene/MWCNT nanocomposite. *Sensors Actuators B Chem* 201:51–58
- Agnieszka B, Anna B, Anna J, Mikołaj K, Jacek W, Marek L, Grzegorz DS (2021) A comparative study of electrocatalytic reduction of hydrogen peroxide at carbon rod electrodes decorated with silver particles. *Mater Sci Eng B* 263:114801
- Chao L, Wang W, Dai M, Ma Y, Sun L, Qin X, Xie Q (2016) Step-by-step electrodeposition of a high-performance Prussian blue-gold nanocomposite for H<sub>2</sub>O<sub>2</sub> sensing and glucose, biosensing. *J Electroanal Chem* 778:66–73
- Chen Y, Li Q, Jiang H, Wang X (2016) Pt modified carbon fiber microelectrode for electrochemically catalytic reduction of hydrogen peroxide and its application in living cell H<sub>2</sub>O<sub>2</sub> detection. *J Electroanal Chem* 781:233–237
- Devasenathipathy R, Kohilarani K, Chen SM, Wang SF, Wang SC, Chen CK (2016) Electrochemical preparation of biomolecule stabilized copper nanoparticles decorated reduced graphene oxide for the sensitive and selective determination of hydrogen peroxide. *Electrochim. Acta* 191:55–61
- Díaz Nieto CH, Granero AM, Lopez JC, Pierini GD, Levin GJ, Fernández H, Zon MA (2018) Development of a third generation biosensor to determine hydrogen peroxide based on a composite of soybean peroxidase/chemically reduced graphene oxide deposited on glassy carbon electrodes. *Sensors Actuators B Chem* 263:377–386
- Doblhofer K (1980) Electrodes covered with thin, permeable polymer films. *Electrochim. Acta* 25(6):871–878
- Du P, Zhou B, Cai C (2008) Development of an amperometric biosensor for glucose based on electrocatalytic reduction of hydrogen peroxide at the single-walled carbon nanotube/Nile blue A nanocomposite modified electrode. *J Electroanal Chem* 614(1):149–156
- Ehsani M, Chaichi MJ, Hosseini SN (2017) Comparison of CuO nanoparticle and CuO/MWCNT nanocomposite for amplification of chemiluminescence immunoassay for detection of the hepatitis B surface antigen in biological samples. *Sensors Actuators B Chem* 247:319–328
- Ensafi AA, Rezaloo F, Rezaei B (2016) Electrochemical sensor based on porous silicon/silver nanocomposite for the determination of hydrogen peroxide. *Sensors Actuators B Chem* 231:239–244
- Guler M, Turkoglu V, Bulut A, Zahmakiran M (2018) Electrochemical sensing of hydrogen peroxide using Pd@Ag bimetallic nanoparticles decorated functionalized reduced graphene oxide. *Electrochim. Acta* 263:118–126

- Hu M, Chen J, Li ZY, Au L, Hartland GV, Li X, Marquez M, Xia Y (2006) Gold nanostructures: engineering their plasmonic properties for biomedical applications. *Chem Soc Rev* 35:1084–1094
- Hu C, Chen X, Hu S (2007a) Water-soluble single-walled carbon nanotubes films: preparation, characterization and applications as electrochemical sensing films. *J Electroanal Chem* 586(1):77–85
- Hu C, Yang C, Hu S (2007b) Hydrophobic adsorption of surfactants on water-soluble carbon nanotubes: a simple approach to improve sensitivity and antifouling capacity of carbon nanotubes-based electrochemical sensors. *Electrochem Commun* 9(1):128–134
- Ihara K, Hasegawa SI, Naito K (2008) The separation of aluminum(III) ions from the aqueous solution on membrane filter using Alizarin Yellow R. *Talanta* 75(4):944–949
- Kardaş F, Beytur M, Akyıldırım O, Yüksek H, Lütüf Yolcu M, Atar N (2017) Electrochemical detection of atrazine in wastewater samples by copper oxide (CuO) nanoparticles ionic liquid modified electrode. *J Mol Liq* 248:360–363
- Liu J, Zhou D, Liu X, Wu K, Wan C (2009) Determination of kojic acid based on the interface enhancement effects of carbon nanotube/alizarin red S modified electrode. *Colloids Surf B: Biointerfaces* 70(1):20–24
- Liu Y, Liu X, Guo ZH, Hu ZH, Xue ZH, Lu X (2017) Horseradish peroxidase supported on porous graphene as a novel sensing platform for detection of hydrogen peroxide in living cells sensitively. *Biosens Bioelectron* 87:101–107
- Lutfullah B, Muhammet G (2019) An ultra-sensitive non-enzymatic hydrogen peroxide sensor based on SiO<sub>2</sub>-APTES supported Au nanoparticles modified glassy carbon electrode. *Progress in Natural Science. Mater Int* 29:390–396
- Marjan SR, Milan ZM, Dirk E, Valentin M (2019) Electrochemistry of hydrogen peroxide reduction reaction on carbon paste electrodes modified by Ag- and Pt-supported carbon microspheres. *J Solid State Electrochem* 23:1257–1267
- Muhammet G, Vedat T, Arif K, Fatih K (2018) A novel nonenzymatic hydrogen peroxide amperometric sensor based on Pd@CeO<sub>2</sub>-NH<sub>2</sub> nanocomposites modified glassy carbon electrode. *Mater Sci Eng C* 90:454–460
- Pandurangan P, Babu R, Narayanan S (2014) Synergetic effect of Prussian blue film with gold nanoparticle graphite-wax composite electrode for the enzyme-free ultrasensitive hydrogen peroxide sensor. *J Solid State Electrochem* 18:883–891
- Parthasarathy S, Nandhini V, Jeyaprakash BG (2016) Improved sensing response of photo activated ZnO thin film for hydrogen peroxide detection. *J Colloid Interface Sci* 482:81–88
- Priyanga N, Sahaya R, Mehboobali P, Al-Sehemi AG, Siew-Moi P, Yang X, Shu-Y T, Annaraj J, Sambathkumar S, Gnanakumar G (2021) Hierarchical MnS@MoS<sub>2</sub> architectures on tea bag filter paper for flexible, sensitive, and selective non-enzymatic hydrogen peroxide sensors. *J Alloys Compd* 855:157103
- Sahoo S, Sahoob PK, Sudipa M, Satpati AK (2020) A novel low cost nonenzymatic hydrogen peroxide sensor based on CoFe<sub>2</sub>O<sub>4</sub>/CNTs nanocomposite modified electrode. *J Electroanal Chem* 876:114504
- Sheng Q, Yu H, Zheng J (2007) Hydrogen peroxide determination by carbon ceramic electrodes modified with pyrocatechol violet. *Electrochim. Acta* 52(25):7300–7306
- Shobha Jeykumari DR, Narayanan SS (2008) A novel nanobiocomposite based glucose biosensor using neutral red functionalized carbon nanotubes. *Biosens Bioelectron* 23(9):1404–1411
- Shu Y, Li B, Xu Q, Gu P, Xiao X, Liu F, Yu L, Pang H, Hu X (2017) Cube-like CoSn(OH)<sub>6</sub> nanostructure for sensitive electrochemical detection of H<sub>2</sub>O<sub>2</sub> in human serum sample. *Sensors Actuators B* 241:528–533
- Sookhakian M, Zalnezhad E, Alias Y (2017) Layer-by-layer electrodeposited nanowall-like palladium-reduced graphene oxide film as a highly-sensitive electrochemical non-enzymatic sensor. *Sensors Actuators B Chem* 241:1–7
- Thanh TD, Balamurugan J, Lee SH, Kim NH, Lee JH (2016) Novel porous gold-palladium nanoalloy network-supported graphene as an advanced catalyst for non-enzymatic hydrogen peroxide sensing. *Biosens Bioelectron* 85:669–678
- Vesna S, Slađana Đ, Miloš O, Jelena M, Kurt K, Dalibor MS (2020) A novel nonenzymatic hydrogen peroxide amperometric sensor based on AgNp@GNR nanocomposites modified screen-printed carbon electrode. *J Electroanal Chem* 876:114487
- Wang I, Zhu H, Hou H, Zhang Z, Xiao X, Song Y (2011) A novel hydrogen peroxide sensor based on Ag nanoparticles electrodeposited on chitosan-graphene oxide/cysteamine-modified gold electrode. *J Solid State Electrochem* 16:1693–1700
- Wang H, Li T, Ma J, Li K, Zuo X (2017) Silver nanoparticles selectively deposited on graphene-colloidal carbon sphere composites and their application for hydrogen peroxide sensing. *Sensors Actuators B* 239:1205–1212
- Weina X, Jianlin L, Mingjun W, Lin C, Xue W, Chenguo H (2016) Direct growth of MnOOH nanorod arrays on a carbon cloth for high performance non-enzymatic hydrogen peroxide sensing. *Anal Chim Acta* 913:128–136
- Williams RR, Lautenschleger M (1963) Titration of weak acids with tetramethylguanidine as solvent. *Talanta* 10(7):804–808
- Wu K, Hu S (2004) Deposition of a thin film of carbon nanotubes onto a glassy carbon electrode by electropolymerization. *Carbon* 42(15):3237–3242
- Wu ZL, Li CK, Yu JG, Chen XQ (2017) MnO<sub>2</sub>/reduced graphene oxide nanoribbons: facile hydrothermal preparation and their application in amperometric detection of hydrogen peroxide. *Sensors Actuators B Chem* 239:544–552
- Xie Y, Yu Y, Lu L, Ma X, Gong L, Huang X, Liu G, Yu Y (2018) CuO nanoparticles decorated 3D graphene nanocomposite as non-enzymatic electrochemical sensing platform for malathion detection. *J Electroanal Chem* 812:82–89
- Yogeswaran U, Chen SM (2007) Separation and concentration effect of f-MWCNTs on electrocatalytic responses of ascorbic acid, dopamine and uric acid at f-MWCNTs incorporated with poly (neutral red) composite films. *Electrochim Acta* 52(19):5985–5996
- Yue W, Zheng D, Hu C, Hu S (2010) Fabrication and application of poly(alizarin red S)-carbon nanotubes composite film based nitrite sensor. *J Nanosci Nanotechnol* 10(10):6586–6593
- Yusoff N, Rameshkumar P, Mehmood MS, Pandikumar A, Lee HW, Huang NM (2017) Ternary nanohybrid of reduced graphene oxide-nafion@silver nanoparticles for boosting the sensor performance in non-enzymatic amperometric detection of hydrogen peroxide. *Biosens Bioelectron* 87:1020–1028
- Zeng J, Wei W, Wu L, Liu X, Liu K, Li Y (2006) Fabrication of poly(toluidine blue O)/carbon nanotube composite nanowires and its stable low-potential detection of NADH. *J Electroanal Chem* 595(2):152–160
- Zhang R, Chen W (2017) Recent advances in graphene-based nanomaterials for fabricating electrochemical hydrogen peroxide sensors. *Biosens Bioelectron* 89:249–268
- Zhang K, Zhang Y (2010) Label-free electrochemical DNA sensor based on gold nanoparticles/poly(neutral red) modified electrode. *Electroanalysis* 22(6):673–679
- Zhang K, Zhang L, Xu J, Wang C, Geng T, Wang H, Zhu J (2010) A sensitive amperometric hydrogen peroxide sensor based on thionin/EDTA/carbon nanotubes—chitosan composite film modified electrode. *Mikrochim Acta* 171(1):139–144
- Zhang K, Zhang N, Zhang L, Xu J, Wang H, Wang C, Geng T (2011) Amperometric sensing of hydrogen peroxide using a glassy carbon electrode modified with silver nanoparticles on poly(alizarin yellow R). *Mikrochim Acta* 173:135–141